SCIENTIFIC REPORTS

OPEN

SUBJECT AREAS:
INORGANIC CHEMISTRY
PHYSICAL CHEMISTRY
BIOINORGANIC CHEMISTRY
SURFACE CHEMISTRY

Received
16 April 2012

Accepted
25 April 2012

Published
14 May 2012

Correspondence and requests for materials should be addressed to J.M. (j.murakami@aist.go.jp)

Reduction of N_2 by supported tungsten clusters gives a model of the process by nitrogenase

Junichi Murakami[1] & Wataru Yamaguchi[2]

[1]Nanosystem Research Institute, National Institute of Advanced Industrial Science and Technology, Central 5, 1-1-1 Higashi, Tsukuba, Ibaraki 305-8565, Japan, [2]Materials Research Institute for Sustainable Development, National Institute of Advanced Industrial Science and Technology, 2266-98 Anagahora, Shimoshidami, Moriyama, Nagoya 463-8560, Japan.

Metalloenzymes catalyze difficult chemical reactions under mild conditions. Mimicking their functions is a challenging task and it has been investigated using homogeneous systems containing metal complexes. The nitrogenase that converts N_2 to NH_3 under mild conditions is one of such enzymes. Efforts to realize the biological function have continued for more than four decades, which has resulted in several reports of reduction of N_2, ligated to metal complexes in solutions, to NH_3 by protonation under mild conditions. Here, we show that seemingly distinct supported small tungsten clusters in a dry environment reduce N_2 under mild conditions like the nitrogenase. N_2 is reduced to NH_3 via N_2H_4 by addition of neutral H atoms, which agrees with the mechanism recently proposed for the N_2 reduction on the active site of nitrogenase. The process on the supported clusters gives a model of the biological N_2 reduction.

In nature, one finds various metalloenzymes that catalyze difficult and essential chemical reactions under mild conditions[1], which, on the other hand, require high temperature and gas pressure in industry. The enzymes often harness small clusters involving transition metal atoms at their active centers, which are the key materials that enable the difficult chemical reactions. Since metalloenzymes are homogeneous systems working in environments with water, structures and functions of the enzymes have been studied by using metal complexes in solutions.

The well-known and intensively studied example of such enzymes is the nitrogenase. It reduces almost inert N_2 to NH_3 at 300 K and 0.8 atm[2], which is in stark contrast to the industrial Haber-Bosch process that requires harsh conditions like 800 K and 300 atm[3]. Among the nitrogenases, the Mo-dependent nitrogenase[4] is best studied. It carries a complex metal cluster named FeMo cofactor (FeMo-co) with a multicenter core XFe_7MoS_9, where X has been identified as a carbon atom recently[5,6]. The core works as the site for N_2 activation and reduction[4].

The fascinating biological N_2 reduction on nitrogenases has attracted much attention of chemists for more than four decades, which has led to continuing efforts to mimic the function of the enzyme to reduce N_2 to NH_3 under mild conditions. Up to now, NH_3 formation under mild conditions has been reported for metal complexes in solutions[7], including well-defined transition-metal complexes with a N_2 ligand[8–10] and also a nitride[11,12]. These are homogeneous systems basically containing reductants and proton sources in solutions, in which N_2 is reduced by direct transfers of electrons and protons to N_2. The N_2 reduction mechanism is consistent in appearance with the generally accepted Lowe-Thorneley scheme for nitrogenase N_2 reduction which tells us that the biological N_2 reduction proceeds by coupled electron and proton transfers to FeMo-co[13–15].

It has recently been suggested, however, the N_2 activated on FeMo-co is reduced not by the direct electronation/protonation but by addition of neutral H atoms that result from reduction of protons[16–18]: the protons, transferred to FeMo-co presumably through a water-filled channel connecting the surface of proteins surrounding FeMo-co and the cofactor[19–21] are likely to be bound to its sulfur sites[16–18,22,23] and reduced to the H atoms[16–18,23]. This mechanism is needed because the amino acid residue located near the active Fe site of FeMo-co (valine), which works as a "gate keeper" to control access of substrates to the active site[24–26], is hydrophobic and anhydrous and thus it is unlikely that protons gain direct access to N_2[17,18]. This then suggests the N_2 reduction on FeMo-co proceeds in a "dry" environment isolated from H_2O while the whole nitrogenase system functions in an environment with water. This is supported by the X-ray crystallography analysis that the surroundings of the active site of FeMo-co are free from water[2,20,23,26].

Accordingly, following the novel mechanism, the N_2 reduction by FeMo-co comes down to addition of neutral H atoms to N_2 on the metal cluster in a dry environment. This suggests we may be able to mimic the function of nitrogenase if metal clusters are available that enable hydrogenation of N_2 with the H atoms, without recourse to the traditional method using direct protonation in solutions. However, there have been no studies to explore such a possibility.

To examine the possibility, we investigated the N_2 reduction on monodispersed small tungsten clusters (W_n, n=2∼6) fixed on graphite surfaces (see the Methods below and Supplementary Information 1). We have chosen the tungsten cluster because it activates N_2 in molecular form[27] as FeMo-co does and H_2O dissociatively adsorbs on the cluster into H + OH. Consequently, if mixture gas of N_2 and H_2O is fed to the cluster, we have activated N_2 and H atoms coexisting on the cluster. Thus the supported tungsten cluster is an ideal system to check whether such a system can model the biological function of reducing N_2 to NH_3. In the following, we show the system indeed reduces N_2 to NH_3 under mild conditions as nitrogenases.

Results

Figure 1a shows a typical N1s spectrum by X-ray photoelectron spectroscopy (XPS) for N_2 adsorbed by tungsten pentamers (W_5), fixed on a highly-oriented pyrolytic graphite (HOPG) surface at 296 K. It has a peak located at an N1s binding energy (BE) of ∼399.2 eV, which is absent for bare W_5 or a N_2-fed bare HOPG surface. The single peak shows N_2 is adsorbed on the cluster with either a W-N-N-W bridge[27,28] or a η^2- adsorption geometry[29]. Our previous work has shown the total energy of the bridge adsorption geometry is lower than that of the η^2 geometry[30,31] and hence suggests the adsorption with the bridge geometry is more likely. Another notable observation is that no peak is seen around 397.6 eV which is a fingerprint of N atoms resulting from N_2 dissociation[32,33]. We have recently shown N_2 is highly activated in molecular form on the cluster[27,30,31]. The XPS observation in Fig. 1a therefore shows N_2 is bound in an activated molecular form on W_5 at room temperature.

The full width at half maximum of the peak is, however, more than 3 eV, which is larger than that of ∼2.2 eV observed for a single nitrogen species such as N atoms on a bulk W surface. Moreover, the peak seems to have a hump at ∼ 401 eV (the higher BE side of the peak). These observations suggest the peak is not due to N_2 alone but consists of those of a couple of nitrogen species. Since N_2 on the cluster is activated, the other species may be reaction products of N_2 with some adsorbates on the cluster. In the cluster deposition, it was found a few H_2O molecules from the ambient are adsorbed on the clusters and hence they could be the reaction counterpart. To check this, the N1s spectrum was measured for various amounts of adsorbed H_2O. The results given in Figs. 1b and 1c show the shape of the spectrum is very sensitive to the water adsorption: with an increase in the amount of H_2O, the intensity above ∼400 eV becomes large, resulting in a broader spectrum (Fig. 1b) and when more than ∼5 water molecules are adsorbed on the cluster, a single peak becomes distinct at ∼400.8 eV (Fig. 1c). The number of N_2 molecules adsorbed per W_5 was ∼0.1. Considering the experimental conditions (pressure of the N_2 gas, the gas exposure time, the number of clusters on the HOPG surface: see Methods below), the sticking probability of N_2 to the water-adsorbed cluster is ∼ 10^{-5} which is comparable to the initial sticking probability of the dissociative adsorption of N_2 to Fe(111) surface at 300 K[34], which proceeds via a molecular adsorption state with a bridge geometry[28]. The intensity of the peak was substantial only when both N_2 and H_2O are present on the cluster. All these observations suggest the nitrogen species other than N_2 originate from reactions between N_2 and H_2O.

As we have reported, the activated N_2 reacts with O from H_2O to form nitrous oxide (N_2O) at 140 K on the cluster[27]. In the present experiment at room temperature, however, double peaks at 402.6 eV and 406.6 eV, the fingerprint of N_2O, are absent in the N1s XPS spectrum (see Fig. 1c). This is presumably because N_2O, though it may form on the cluster at room temperature, would desorb from the cluster as soon as it forms, since the molecule desorbs from the cluster at ∼ 145 K[27]. Then we have to consider the reaction of N_2 with H which results from dissociative adsorption of H_2O on W_5 (Supplementary Information 2). The calculation given in the supplementary information shows the electron population of the hydrogen for the most stable (H+OH) adsorption configuration on W_5 is 1.1 ∼ 1.2 depending on the model for the population analysis. This indicates the hydrogen is a neutral H atom not a proton as expected. Therefore, the reaction of N_2 with H from H_2O is a process of addition of the neutral H atoms to N_2, which we call "hydrogenation with neutral H atoms" hereafter. Accordingly, the XPS spectral changes in Figs. 1a to 1c may show progress of the hydrogenation of N_2 at room temperature with an increase in the number of coadsorbed H atoms, leading to NH_3 formation.

In an experiment to purposely feed NH_3 to W_5, the molecule was found to give an XPS spectrum with a single peak at 400.4 eV. Therefore, the nitrogen species that give the XPS spectrum in Fig. 1c may include NH_3. To examine this, we analyzed gases desorbing upon heating from W_5, to which N_2 and H_2O were simultaneously fed at 296 K (denoted as (N_2 + H_2O)/W_5) hereafter), by mass spectrometry. For the analysis, we first performed an experiment using $^{15}N_2$, hoping that we could detect $^{15}NH_3$. The experiment turned out to give a hint of ammonia formation but not in an unambiguous way. This is because the mass to charge ratio (m/e) of $^{15}NH_3^+$ is the same as that of $H_2{}^{16}O^+$ (m/e=18) and the major cracked species from these species, $^{15}NH_2^+$ and $^{16}OH^+$, also have the same m/e of 17. Thus the peaks due to desorption of $^{15}NH_3$ from the cluster totally overlap with those of $H_2{}^{16}O$, which is a species always found in an ultrahigh vacuum ambient and also desorbs upon heating from W_5 concomitantly with the ammonia as shown below, in the mass spectrum. We therefore have chosen to use the combination of $^{14}N_2$ and $H_2{}^{18}O$ to have a conclusive result. With this combination one can keep the intensities of $H_2{}^{16}O^+$ and $^{16}OH^+$ almost to the background level as seen in Fig.2a: comparison of the intensity for m/e=17 with that of the $H_2{}^{16}O^+$ peak should

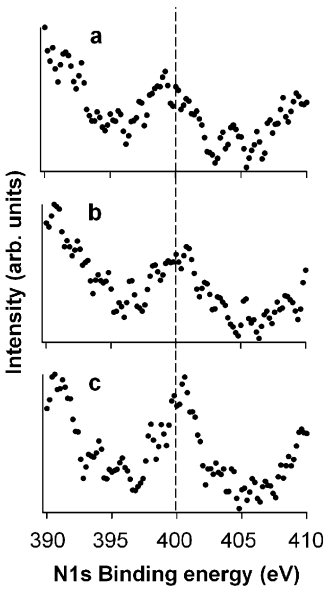

Figure 1 | Dependence of the N1s XPS spectral shape for N_2/W_5 at 296 K on the amount of chemisorbed H_2O. The average number of chemisorbed H_2O molecules per W_5 for (a), (b) and (c) was 2.2, 3.4 and 5.5, respectively. These numbers were deduced from the relative XPS peak intensity of O1s for chemisorbed H_2O to that of $W4p_{3/2}$, taking account of the photoionization cross sections of these lines for the MgKα X-ray used in XPS. The vertical line at 400 eV BE is a guide for an eye.

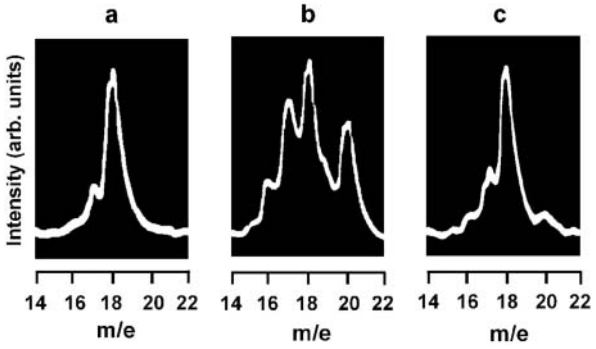

Figure 2 | Mass spectra for thermal desorption of surface species from $(N_2+H_2{}^{18}O)/W_5$. At (a) 296 K, (b) ~320K and (c) ~350 K.

make the desorption of $^{14}NH_3$ easily noticeable. Before heating the sample of $(^{14}N_2 + H_2{}^{18}O)/W_5$, XPS measurement was carried out to confirm that the spectrum was dominated by the peak at 400.8 eV. Figure 2a shows a mass spectrum measured before the sample is heated. It is a background mass spectrum owing to H_2O in the ultra-high vacuum ambient of the mass spectrometer chamber. The peak at m/e=18 is due to $H_2{}^{16}O^+$ and the shoulder at m/e=17 with ~ 1/3 intensity of $H_2{}^{16}O^+$ is due to $^{16}OH^+$ that results from cracking of $H_2{}^{16}O$. When the sample is heated to ~320 K, we observed dramatic changes in the mass spectrum (Fig. 2b): three peaks with m/e of 16, 17 and 20, absent in the background spectrum, showed up. Since the intensity of the m/e=17 peak is comparable to that of the $H_2{}^{16}O^+$ peak (m/e=18), it is apparently not solely due to $^{16}OH^+$ but includes a substantial intensity of another species and it is $^{14}NH_3{}^+$:$^{14}NH_3{}^+$ is the only possible chemical species with m/e =17 other than$^{16}OH^+$ for possible combinations of ^{14}N, ^{16}O, and H. We also notice substantial intensity increase for the peak with m/e=16, which we assign to $^{14}NH_2{}^+$ that results from cracking of $^{14}NH_3$. The assignment is consistent with the previous report that $NH_3{}^+$ and $NH_2{}^+$ are the major species (the intensity of $NH_2{}^+$ is ~0.5 of that of $NH_3{}^+$) when NH_3 is analyzed by a quadrupole mass spectrometer[35]. The peak at m/e=20 is assigned to $H_2{}^{18}O^+$ that was fed to the cluster. After the gas desorption, the mass spectrum became similar to that prior to the heating (Fig. 2c). The desorption of NH_3 was observed in the same manner without the prior XPS measurement, indicating the formation of NH_3 is not induced by X-ray radiation. Thus the mass spectra give conclusive evidence that NH_3 forms from N_2 and H atoms originated from dissociative adsorption of H_2O on supported W_5.

As mentioned above, N_2 is activated in molecular form on W_5. Hence the N_2 hydrogenation may proceed by addition of H atoms to N_2, yielding intermediate hydrazine-like species N_2H_x (x=1~4). To examine the possibility of such a process and the existence of hydrogenated species, we measured the N1s XPS spectrum of hydrazine monohydrate ($N_2H_4{\cdot}H_2O$) purposely fed to W_5 (N_2H_4/W_5, Fig. 3a) and compared it with the spectrum for $(N_2 + H_2O)/W_5$ at 296 K (Fig. 3b). We also compared XPS spectra for the two systems after they were heated to 380 K (Fig. 3c for N_2H_4/W_5 and Fig. 3d for $(N_2 + H_2O)/W_5$). As is readily noticed, the XPS spectra for $(N_2 + H_2O)/W_5$) bear striking resemblance to those for N_2H_4/W_5. Although the signal to noise ratio for the former is much smaller than that for the latter owing to the small number of N_2 adsorbed on W_5, it is evident for the Goth systems that (1) the main peak is located at ~400.8eV and a shoulder at ~398.4 eV before the heat treatment; (2) after being heated to 380 K, the intensity above 400 eV decreases whereas the intensity below 400 eV increases; (3) the total nitrogen intensity decreases by the heat treatment, indicating a fraction of the species responsible for the main peak desorbed. This observation that the XPS spectra of the two systems have common features in many respects strongly indicates similar hydrogenated nitrogen species exist in N_2H_4/W_5 and $(N_2+H_2O)/W_5$ and this means N_2 in $(N_2+H_2O)/W_5$ is hydrogenated, i.e., reduced at room temperature. As noted above NH_3 gives the XPS spectrum with the peak energy of 400.4 eV. Thus the observation (1) indicates the presence of a species with the binding energy larger than that of NH_3 for the both systems.

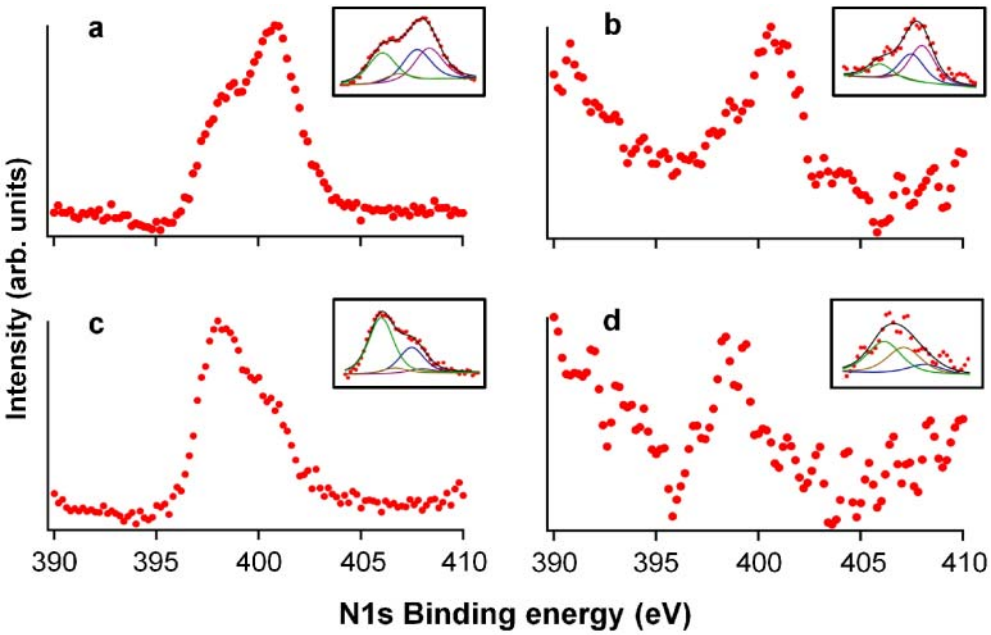

Figure 3 | XPS spectra in the N1s region. (a) N_2H_4/W_5 and (b) $(N_2+H_2O)/W_5$, at 296 K and (c) N_2H_4/W_5 and (d) $(N_2+H_2O)/W_5$ after being heated to 380 K. The peak heights are adjusted to the full scale of the vertical axes. The initial number of N_2H_4 molecules per cluster is ~2 for N_2H_4/W_5 and that of N_2 is ~0.1 for $(N_2 + H_2O)/W_5$). This is the reason for the much smaller signal to noise ratio of the spectra for $(N_2+H_2O)/W_5$ compared to those for N_2H_4/W_5. For the both systems the total N1s intensity after the heat treatment was reduced to ~60 % of the initial intensity. In the insets red dots give the experimental result and solid lines the results of the analysis, which revealed four species at 398.1 eV (NH, denoted in green), 399.2 eV (N_2, brown), 400.4 eV (NH_3, blue) and 401.2 eV (N_2H_4, purple). The black solid line is the sum of the peaks of all the components.

To identify the hidden hydrogenated species, we carried out factor analysis first for the spectra of N_2H_4/W_5 (Fig. 3a and Fig. 3c) because they have large signal to noise ratios tolerable for the analysis. We then used the result of the analysis for examining the spectra for $(N_2 + H_2O)/W_5$. The result of the factor analysis is given by solid lines in the inset of Fig. 3a. As seen in the inset, the experiment (red dots) is well reproduced by the analysis (the black solid line) if four species with the BEs of 398.1 eV, 399.2 eV, 400.4 eV and 401.2 eV are assumed. The factor analysis including the four species also well explains the spectrum after the heat treatment (the inset of Fig.3c). Previous studies dealing with N_2H_4 adsorption on metal surfaces[35–38] and supported metal clusters[39] have shown the molecule is adsorbed intact at low temperatures but easily dissociates at elevated temperatures to yield N_2H_x(x=1∼3), NH_y (y=1∼3), N, N_2 and H_2. The literature suggests the species with the BE of 398.1 eV is NH[33] and there is no sign of nitrides (the BE = 397.6 eV). The species with the BE of 399.2 eV is probably N_2 as suggested from Fig.1a. The peak at 400.4 eV is assigned to NH_3 because the BE matches the N1s peak energy of the NH_3 XPS spectrum. The peak intensities of NH_3 and the species at 401.2eV decrease by heating, which concomitantly occurs with the intensity increase of NH (compare the insets of Fig. 3a and Fig. 3c) and the decrease of the total nitrogen intensity. Similar intensity changes of the species were observed even at room temperature as will be described below. These observations can be understood as a result of decomposition of the species at 401.2eV to NH and desorbing NH_3 and hence suggests it is N_2H_x (x=1∼4). It is notable that the peaks due to NH and NH_3 already have substantial intensities before the heating (Fig.3a inset). This can be explained by immediate decomposition upon adsorption of the N_2H_4 molecule that arrives first to W_5, which is a reaction with large exothemicity[37]. Since the decomposition pattern of N_2H_x upon heating mentioned above is similar to that of N_2H_4, it is strongly suggested the N_2H_x is due mainly to N_2H_4. N_2H_4 observed in the spectrum in Fig. 3a is probably the molecule that arrived later at the cluster and was stabilized by preadsorbed N_2H_4[36]. The peak assignments are supported by thermal desorption spectroscopy (TDS) for N_2H_4/W_5 which shows desorptions of NH_3 and N_2H_4 upon heating the system (Supplementary Information 3): this is consistent with the finding by the XPS spectra that the intensities of the N_2H_4 and NH_3 peaks greatly decrease upon heating.

Then we examined the spectrum for $(N_2 + H_2O)/W_5$ at 296 K (Fig. 3b) and that after heating to 380 K (Fig. 3d). As mentioned above, the XPS spectra for $(N_2 + H_2O)/W_5$ bear striking resemblance to those for N_2H_4/W_5. In accordance with this, the factor analysis with the above four species, i.e., NH, N_2, NH_3 and N_2H_4, can explain the observed spectrum at 296 K rather well (Fig.3b inset). As seen in the inset, the intensity of the N_2 peak is much smaller than those of the NH, NH_3 and N_2H_4 peaks as in N_2H_4/W_5. Since NH and NH_3 result from decomposition of N_2H_4 on W_5 as mentioned above, the finding suggests that N_2, once activated by W_5, is readily hydrogenated down to N_2H_4, which then decomposes to NH_3 and NH: it is seen from Fig. 3b inset that most of the N_2 molecule coadsorbed with H_2O on W_5 are hydrogenated to N_2H_4 and nearly half of N_2H_4 are converted to NH and NH_3 at room temperature. The facile formation of N_2H_4 from N_2 is consistent with the theoretical calculation that it is an exothermic process after the first addition of H[40]. The observed changes in the spectral shape and intensity upon heating (the observations (2) and (3) above, compare Fig. 3b with Fig. 3d) can be explained by the decomposition of N_2H_4 to NH and NH_3 and the desorption of the latter. This is consistent with the observation of NH_3 by TDS shown in Fig. 2b. However, the desorption of N_2H_4, observed for N_2H_4/W_5 by TDS, was not found for $(N_2 + H_2O)/W_5$. A possible explanation for this is that N_2H_4 on the clusters are all subjected to reaction upon heating with the surface H atoms that are more abundant for $(N_2 + H_2O)/W_5$ than in N_2H_4/W_5. It is notable that N_2H_4 cracks to yield NH_3^+ by electron bombardment in a mass spectrometer with the intensity of ≤ 0.5 of that of $N_2H_4^+$[35,37]. We checked the cracking of N_2H_4 by monitoring a mass spectrum while admitting N_2H_4•H_2O into the vacuum chamber and found that the most prominent species was $N_2H_4^+$. The finding that N_2H_4 desorption was not observed for $(N_2+H_2O)/W_5$ therefore suggests that the observation of NH_3 shown in Fig. 2b is not due to cracking of desorbed N_2H_4 and thus the NH_3 molecule had formed on the cluster before it desorbed.

In the experiments described above, we have focused on W_5 but it is not the only tungsten cluster to adsorb and activate N_2 in a bridge geometry. The 1st principles calculations for isolated tungsten clusters show W_4 and W_6 are also capable of similar N_2 activation[31]. In accordance with this, these clusters gave the N1s peak at 400.8 eV in XPS spectra, indicating the formation of the hydrogenated nitrogen species. Surprisingly, the formation of the hydrogenated species was also found for W_2 and W_3, which do not support such stable bridge adsorptions of N_2[31]. It was found by calculation, however, that water adsorption stabilizes N_2 bridge adsorption on the clusters (Supplementary Information 4 online), which may have enabled the clusters to mediate the formation of the hydrogenated nitrogen species.

Discussion

The results described above are summarized as follows: supported small tungsten clusters activate N_2 in molecular form and convert the molecule to NH_3 via N_2H_4 at room temperature. The N_2 reduction is done by hydrogenation with neutral H atoms on the cluster, which is distinct from the mechanism of the traditional N_2 reduction using electronation and protonation in solutions. The hydrogenation mechanism is similar to those proposed for FeMo-co[17,18,23] of the nitrogenase and thus gives support to them.

It is interesting to note that in biochemical experiments dealing with nitrogenases N_2H_4 is suggested as a N_2 reduction intermediate[41]. Thus, the present cluster system and nitrogenase convert N_2 to NH_3 via the common intermediate. The formation of N_2H_4 means both N atoms of N_2 are hydrogenated before the cleavage of the N-N bond. This is consistent with the observation in the present experiment by the XPS spectra in Fig.3b and 3d that show no sign of N atom formation and is called the "alternative mechanism" for the N_2 reduction by nitrogenase that is theoretically[18,42] and experimentally[43,44] thought likely to be the case.

Since the N_2 reduction by W_5 proceeds in a manner similar to those proposed for the FeMo-co of nitrogenase, findings on the reduction process on the cluster may shed light on the long-standing mysteries in the mechanism of the biological N_2 reduction how the robust N-N triple bond of N_2 cleaves[45] and why the N_2 reduction to NH_3 easily occurs at room temperature[17]. As discussed above, N_2H_4 is the N_2 reduction intermediate for the present cluster system and also suggested as an intermediate for the biological systems. N_2H_4 is an intrinsically unstable molecule with the free energy of formation of 38.07 Kcal/mol and the N-N bond easily cleaves on metal surfaces as mentioned above. The instability of N_2H_4 at room temperature on W_5 is evidenced by the time evolution of the XPS spectrum for N_2H_4/W_5 at 296 K shown in Figs. 4a to 4c. As seen in the figures, the shoulder at ∼398.0 eV gradually grows bigger compared to the the peak at ∼400.8 eV. This is due to gradual intensity decreases of N_2H_4 and NH_3 with concomitant intensity increase of NH as seen in the insets of Fig. 4, which is summarized in Fig. 4d. The intensity decrease of N_2H_4 with time indicates the N-N bond of the species is unstable on the cluster at room temperature and cleaves to yield NH and NH_3 as mentioned above. The resultant NH_3 gradually desorbs from the cluster, which explains the decreases in the total N1s and NH_3 intensities shown in Fig. 4d. It is likely N_2H_4 is also unstable and reactive on the CFe_7MoS_9 cluster of FeMo-co at ambient temperature as on W_5 and therefore, once it forms, its N-N bond easily cleaves, leading to the formation and the subsequent

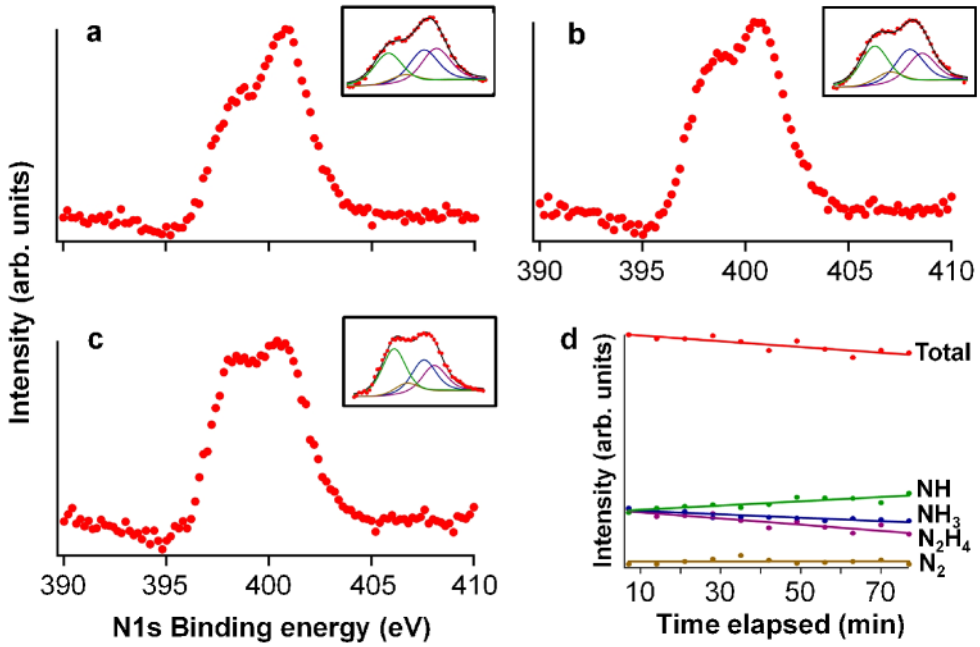

Figure 4 | Evolution of the N1s XPS spectra for $(N_2+H_4)/W_5$ at 296 K with time. The spectra were measured at (a) 7 min, (b) 40 min and (c) 80 min after feeding $N_2H_4 \cdot H_2O$ to W_5. The notations for the insets are the same as those in Fig. 3. The XPS spectral changes depend on the time elapsed after feeding $N_2H_4 \cdot H_2O$ to the cluster but not on the time spent for the XPS measurement, indicating they are spontaneous changes and not induced by the X-ray radiation. (d) N1s intensity changes of each species with time. The intensity of each species is the area for each peak deduced from the factor analysis of the XPS spectrum. The lines in the graph are the results of curve fitting of the data points.

desorption of NH_3. The formation of the intermediate species, N_2H_4 is a consequence of the N_2 activation in molecular form and thus this mode of N_2 activation by FeMo-co is the key to the biological NH_3 formation from N_2 under mild conditions.

We have shown supported small tungsten clusters reduce N_2 to NH_3 under mild conditions as nitrogenases do. N_2 is reduced to NH_3 via N_2H_4 by hydrogenation with neutral H atoms in a dry environment. The N_2 hydrogenation mechanism is consistent with and thus gives support to the recently-proposed model that N_2 is reduced by hydrogenation on the active site of nitrogenase, FeMo-co, with H atoms resulting from reduction of protons. The overall mechanism of the N_2 reduction to NH_3 by the tungsten cluster is similar to those proposed for the N_2 reduction of nitrogenase and thus the process on the supported clusters gives a model of the biological N_2 reduction. The key material common to the enzyme in nature and in the present study is the small metal cluster that can activate N_2 in molecular form, which leads to the NH_3 formation at room temperature. In nature, small metal clusters in various metalloenzymes are known to work being isolated from water[1] as FeMo-co and thus, if appropriate metal clusters are available, they may be used in dry environments to mimic the functions of the enzymes.

Methods

Generation, deposition and fixation of size-selected tungsten clusters on a highly-oriented pyrolytic graphite (HOPG) surface. Tungsten cluster ions (W_n^+, n=2~6), sputtered from W plates by high-energy (~23 kV) Xe^+ ion beams, were cooled by collision with helium gas and size-selected by a quadrupole mass-filter and then deposited on an HOPG surface at 296 K. The cluster beam has a mean kinetic energy of ~2.5 eV to the surface and is decelerated by applying a positive voltage with the same magnitude to the substrate. By doing this, kinetic energies of the cluster ions incident to the surface is reduced to less than ~0.3 eV/cluster[46], making them "soft land" on the surface. The number of the incident clusters was typically $2.3 \times 10^{13,32}$. Since W-W bond energy (e.g., ~5 eV for W_2) is much larger than the incident energy, it is ensured that the clusters are non-destructively deposited. Prior to the cluster deposition, the HOPG surface was bombarded by an Ar^+ ion beam with a collision energy of 50 eV. This creates defects on its outermost surface[47] that work for anchoring the clusters separately[48].

Measurement and analysis of chemical reactions on the clusters. Size-selected W_n (n=2~6), supported on an HOPG substrate at 296 K, were exposed to excessive amount of N_2 (99.9999 % purity) or a mixture of the N_2 plus degassed H_2O (distilled water or ultrapure water for ultratrace analysis) or water-^{18}O (^{18}O content 95–98 %) from a pulsed valve or an all-metal leak valve. The exposure to N_2 was performed with an ion gauge off to prevent adsorption of excited N_2 on the clusters. Typically the N_2 pressure was $\sim 10^{-4}$ Torr and the exposure time was 90 sec. $N_2H_4 \cdot H_2O$ (98 % purity)was fed to the clusters also with an ion gauge off through a needle valve with a doser made of glass to prevent cracking of the molecule. XPS was done using MgXα (1253.6 eV) X-rays and a hemispherical electron energy analyzer. The factor analysis of XPS spectra was performed using the program XPSPEAK ver. 4.1 (http://www.kwoksys.com/). To obtain mass spectra of desorbing gases with a substantial signal to noise ratio, the gases were fed through the all-metal leak valve heated to ~400 K: this procedure gave XPS spectra identical to that in Fig. 1c but with enhanced intensity. The effect of heating the gas is possibly to increase the fraction of the N_2 molecules that overcome the barrier for the bridge adsorption state[34,49]. In measuring mass spectra of thermally desorbing gases, the substrate was heated with a constant temperature rise of ~8 K/sec by electron bombardment using a tungsten filament located at the back of the substrate. The substrate temperature was monitored with an alumel-chromel thermocouple. Desorbed species were analyzed by a quadrupole mass spectrometer and the resulting mass spectra were monitored by an oscilloscope. A movie was taken by a digital camera to record the changes of the resulting mass spectra with the rise of the substrate temperature. The mass spectra in Fig. 2 are the snap shots from a movie recording mass spectrum changes by heating the sample from 300 K to 400 K. All the experiments were done in a stainless-steel vacuum chamber with a base pressure of low 10^{-10} Torr.

1. Lippard, S. J. & Berg, J. M. *Principles of Bioinorganic Chemistry* (Univ. Science Books, Herndon, 1997).
2. Howard, J. B. & Rees, D. C. Structural basis of biological nitrogen fixation. *Chem. Rev.* **96**, 2965–2982(1996).
3. Schlögl, R. Catalytic synthesis of ammonia - a "never-ending story"? *Angew. Chem. Int. Ed.* **42**, 2004–2008(2003).
4. Burgess, B. K. & Lowe, D. J. Mechanism of molybdenum nitrogenase. *Chem. Rev.* **96**, 2983–3011(1996).
5. Spatzal *et al.* Evidence for interstitial carbon in nitrogenase FeMo cofactor. *Science* **334**, 940 (2011).
6. Lancaster, K. M. *et al.* X-ray emission spectroscopy evidences a central carbon in the nitrogenase iron-molybdenum cofactor. *Science* **334**, 974–977 (2011).
7. Shilov, A. E. Catalytic reduction of dinitrogen in protic media: chemical models of nitrogenase. *Mol. Catal.* **41**, 221 (1987).
8. Yandulov, D. M. & Schrock, R. R. Catalytic reduction of dinitrogen to ammonia at a single molybdenum center. *Science* **301**, 76 (2003).

9. Gilbertson, J. D., Szymczak, N. K. & Tyler, D. R. Reduction of N_2 to ammonia and hydrazine utilizing H_2 as the reductant. *J. Am. Chem. Soc.* **127**, 10184–10185 (2007).
10. Arashiba, K., Miyake, Y. & Y. Nishibayashi. A molybdenum complex bearing PNP-type pincer ligands leads to the catalytic reduction into ammonia. *Nat. Chem.* **3**, 120 (2011).
11. Scepaniak, J. J. *et al*. Synthesis, structure, and reactivity of an iron(V) nitride. *Science* **331**, 1049 (2011).
12. Askevold, B. *et al*. Ammonia formation by metal–ligand cooperative hydrogenolysis of a nitrido ligand. *Nat. Chem.* **3**, 532–537 (2011).
13. Lowe, D. J. & Thorneley, R. N. F. The mechanism of *Klebsiella pneumoniae* nitrogenase action. Pre-steady-state kinetics of H_2 formation. *Biochem. J.* **224**, 877–886 (1984).
14. Thorneley, R. N. F. & Lowe, D. J. The mechanism of *Klebsiella pneumoniae* nitrogenase action. Pre-steady-state kinetics of an enzyme-bound intermediate in N_2 reduction and of NH_3 formation. *Biochem. J.* **224**, 887–894 (1984).
15. Lowe, D. J. & Thorneley, R. N. F. The mechanism of *Klebsiella pneumoniae* nitrogenase action. The determination of rate constants required for the simulation of the kinetics of N_2 reduction and H_2 evolution. *Biochem. J.* **224**, 895–901 (1984).
16. Dance, I. The hydrogen chemistry of the FeMo-co active site of nitrogenase. *J. Am. Chem. Soc.* **127**, 10925–10942 (2005).
17. Dance, I. Elucidating the coordination chemistry and mechanism of biological nitrogen fixation. *Chem. Asian. J.* **2**, 936 (2007).
18. Dance, I. The chemical mechanism of nitrogenase: calculated details of the intramolecular mechanism for hydrogenation of η^2-N_2 on FeMo-co to NH_3. *Dalton Trans.* 5977–5991 (2008).
19. Szilagyi, R. K., Musaev, D. G. & Morokuma, K. Theoretical studies of biological nitrogen fixation. Part II. Hydrogen bonded networks as possible reactant and product channels. *J. Mol. Struct. (Theochem.)* **506**, 131–146 (2000).
20. Durrant, M. C. Controlled protonation of iron-molybdenum cofactor by nitrogenase: a structural and theoretical analysis. *Biochem. J.* **355**, 569–576 (2001).
21. Schimpl, J., Petrilli, H. M. & Blöchl, P. E. Nitrogen binding to the FeMo-cofactor of nitrogenase. *J. Am. Chem. Soc.* **125**, 15772–15778 (2003).
22. Siegbahn, P. E. M., Westerberg, J., Svensson, M. & Crabtree, R. H. Nitrogen fixation by nitrogenases: a quantum chemical study. *J. Phys. Chem.* **102**, 1615 (1998).
23. Hinnemann, B. & Nørskov, J. K. Catalysis by enzymes: the biological ammonia synthesis. *Top. in Catal.* **37**, 55–70 (2006).
24. Benton, P. M. C. *et al*. Localization of a substrate binding site on the FeMo-cofactor in nitrogenase: trapping propargyl alcohol with an α-70-substituted MoFe protein. *Biochemistry* **42**, 9102–9109 (2003).
25. Seefeldt, L. C., Seefeldt, L. C., Hoffman, B. M. & Dean, D. R. Mechanism of Mo-Dependent Nitrogenase. *Annu. Rev. Biochem.* **78**, 701–722 (2009).
26. Sarma, R. *et al*. Insights into substrate binding at FeMo-cofactor in nitrogenase from the structure of an α-70^{Ile} MoFe protein variant. *J. Inor. Biochem.* **104**, 385 (2010).
27. Yamaguchi, W. & Murakami, J. Low temperature formation of nitrous oxide from dinitrogen, mediated by supported tungsten nanoclusters. *J. Am. Chem. Soc.* **129**, 6102–6103 (2007).
28. Raval, R., Harrison, M. A. & King, D. A. Nitrogen adsorption on metals. in *The Chemical Physics of Solid Surfaces and Heterogeneous Catalysis vol.2: Adsorptions at Solid Surfaces*(eds. King, D. A & Woodruff, D. P.) 39–129 (Elsevier, Amsterdam, 1982).
29. Grunze, M. *et al*. π-bonded N_2 on Fe(111): the precursor for dissociation. *Phys. Rev. Lett.* **53**, 850–853 (1984).
30. Yamaguchi, W. & Murakami, J. A computational study on molecular adsorption states of nitrogen on a tungsten tetramer. *Phys. Chem. Chem. Phys.* **11**, 943 (2009).
31. Yamaguchi, W. & Murakami, J. Adsorption states of dinitrogen on small tungsten nanoclusters. *Chem. Phys. Lett.* **455**, 261–264 (2008).
32. Yamaguchi, W. & Murakami, J. Nitrogen adsorption on supported size-selected tungsten nanoclusters as studied by X-ray photoelectron and X-ray Auger electron spectroscopies. *Chem. Phys. Lett.* **378**, 521–525 (2003).
33. Grunze, M., Brundle, C. R. & Tománek, D. Adsorption and decomposition of ammonia on a W(110) surface: photoemission fingerprinting and interpretation of the core level binding energies using the equivalent core approximation. *Surf. Sci.* **119**, 133–149 (1982).
34. Rettner, C. T. & Stein, H. Effect of translational energy on the chemisorption of N_2 on Fe(111): activated dissociation via a precursor state. *Phys.Rev.Lett.* **59**, 2768–2771(1987).
35. Al-Haydari, Y. K., Saleh, J. M. & Matloob, M. H. Adsorption and decomposition of hydrazine on metal films of iron, nickel, and copper. *J. Phys. Chem.* **89**, 3286–3290 (1985).
36. Grunze, M. The interaction of hydrazine with an Fe(111) surface. *Surf. Sci.* **81**, 603–625 (1979).
37. Dopheide, R., Schröter, L. & Zacharias, H. Adsorption and decomposition of hydrazine on Pd(100). *Surf. Sci.* **257**, 86–96 (1991).
38. Rauscher, H., Kostov, K. L. & Menzel, D. Adsorption and decomposition of hydrazine on Ru(111). *Chem. Phys.* **177**, 473–496(1993).
39. Fan, C., Wu, T., Kaden, W. E. & Anderson, S. L. Cluster size effects on hydrazine decomposition on Ir_n/Al_2O_3/NiAl(110). *Surf. Sci.* **600**, 461–467 (2005).
40. Rod, T. H., Lagadottir, A. & Nørskov, J. K. Ammonia synthesis at low temperatures. *J. Chem. Phys.* **112**, 5343–5347 (2000).
41. Barney, B. M. *et al*. Trapping a hydrazine reduction intermediate on the nitrogenase active site. *Biochemistry* **44**, 8030 (2005).
42. Kästner, J & Blöchl, P. E. Ammonia production at the FeMo cofactor of nitrogenase: results from density functional theory. *J. Am. Chem. Soc.* **129**, 2998–3006 (2007).
43. Barney, B. M. *et al*. A methyldiazene ($HN{=}N{-}CH_3$)-derived species bound to the nitrogenase active-site FeMo cofactor: implications for mechanism. *Proc. Nat. Acad. Sci.* **103**, 17113–17118 (2006).
44. Hoffman, B. M., Dean, D. R. & Seefeldt, L. C. Climbing nitrogenase: toward a mechanism of enzymatic nitrogen fixation. *Acc. Chem. Res.* **42**, 609–619 (2009).
45. Barney, B. M. *et al*. Breaking the N_2 triple bond: insights into the nitrogenase mechanism. *Dalton Trans.* 2277–2284 (2007).
46. Yamaguchi, W. *et al*. Energy-controlled depositions of size-selected silver nanoparticles on HOPG substrates. *Chem. Phys. Lett.* **311**, 341–345 (1999).
47. Marton, D. *et al*. Near-threshold ion-induced defect production in graphite. *Phys. Rev. B* **48**, 6757–6766 (1993).
48. Vijayakrishnan, V. & Rao, C. N. R. An investigation of transition metal clusters deposited on graphite and metal oxide substrates by a combined use of XPS, UPS and Auger spectroscopy. *Surf. Sci.* **255**, L516–L522 (1991).
49. Grunze, M., Strasser, G. & Golze, M. Precursor mediated and direct adsorption of molecular nitrogen on Fe(111). *Appl. Phys. A* **44**, 19–29 (1987).

Acknowledgements

We are grateful to S. L. Anderson and Y. Norikane for their advice on handling hydrazine. We also thank M. Yokoi for his help in solving the operation problems of the quadrupole mass systems of the cluster machine.

Author contributions

J. M. designed and performed the experiments and analyzed the data. W.Y. constructed data acquisition systems for thermal desorption spectroscopy and also performed the DFT calculations. Both contributed to writing the paper.

Additional information

Supplementary information accompanies this paper at http://www.nature.com/scientificreports

Competing financial interests: The authors declare no competing financial interests.

Reprints and permission information is available online at http://npg.nature.com/reprintsandpermissions/

How to cite this article: Murakami, J. & Yamaguchi, W. Reduction of N_2 by supported tungsten clusters gives a model of the process by nitrogenase. *Sci. Rep.* **2**, 407; DOI:10.1038/srep00407 (2012).